Solution Chemistry of Self-Assembled Graphene Nanohybrids for High-Performance Flexible Biosensors

ARTICLE *in* ACS NANO · APRIL 2010

Impact Factor: 12.88 · DOI: 10.1021/nn100145x · Source: PubMed

Supporting Information

Solution Chemistry of Self Assembled Graphene Nanohybrids for High Performance Flexible Biosensors

Bong Gill Choi,[†] HoSeok Park,[‡,] Tae Jung Park,[§] Min Ho Yang,[†] Joon Sung Kim,[¶] Sung-Yeon Jang,[¶] Nam Su Heo,[§] Sang Yup Lee,[†, §] Jing Kong,[⊥] and Won Hi Hong[†,]**

[†]Department of Chemical & Biomolecular Engineering (BK21 program), KAIST, Daejeon 305-701, Korea

[‡]Department of Chemical Engineering, College of Engineering, Kyung Hee University, 1 Seochon, Giheung, Yongin, Gyeonggi 446-701, Korea

[§]BioProcess Engineering Research Center, Center for Systems & Synthetic Biotechnology, and Institute for the BioCentury, KAIST, Daejeon 305-701, Korea

[¶]Center for Energy Materials Research, Korea Institute of Science and Technology, P.O. Box 131 Cheongryang, Seoul 130-650, Korea

[⊥]Department of Electrical Engineering and Computer Sciences, and

Department of Physics, Massachusetts Institute of Technology, Cambridge, Massachusetts 02139

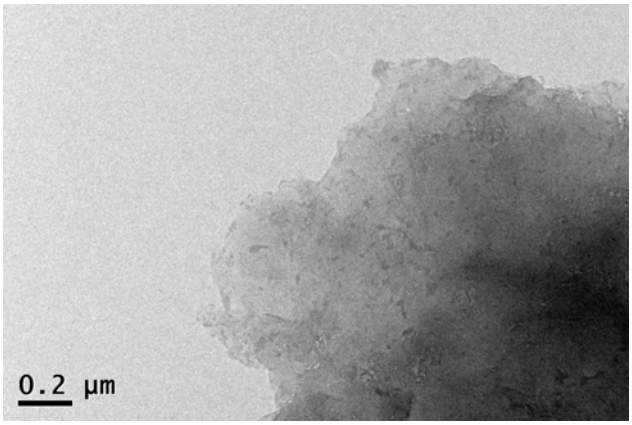

Figure S1. TEM image of GON.

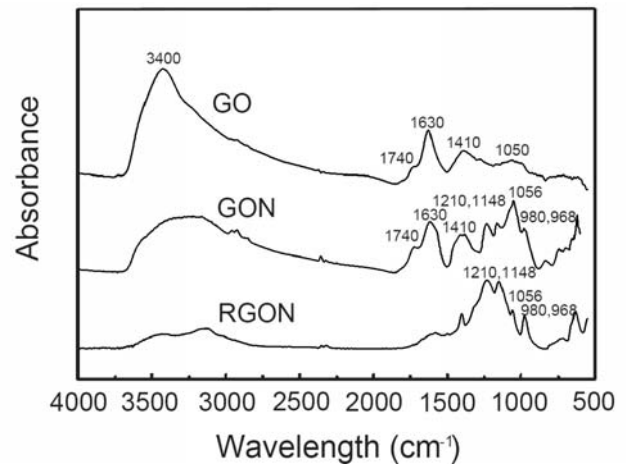

Figure S2. FT-IR spectrum of the GO, GON, and the RGON hybrid.

FT-IR results demonstrate the presence of Nafion in GON and RGON. The characteristic bands of GO were assigned to 3400 cm^{-1} for ν_{O-H}, 1740 cm^{-1} for $\nu_{C=O}$, 1630 cm^{-1} for $\nu_{adsorbed\ H2O}$, 1410 cm^{-1} for $\nu_{O-H\ deform}$, and 1050 cm^{-1} for $\nu_{C-O\ stretch.}$.[1] The characteristic bands of Nafion were assigned to 1210 cm^{-1} for $\nu_{asym.\ CF2}$, 1148 cm^{-1} for $\nu_{sym.\ CF2}$, 1056 cm^{-1} for $\nu_{S=O}$, and 980 cm^{-1} and 968 cm^{-1} for ν_{C-O-C}. The characteristic bands of the Nafion in GON appeared when the GOs were coated with the Nafion by the sonic treatment. After the reduction of GON to RGO in the presence of the Nafion, RGON revealed a lower intensity of the characteristic bands of GO and a higher intensity of the characteristic bands of Nafion.

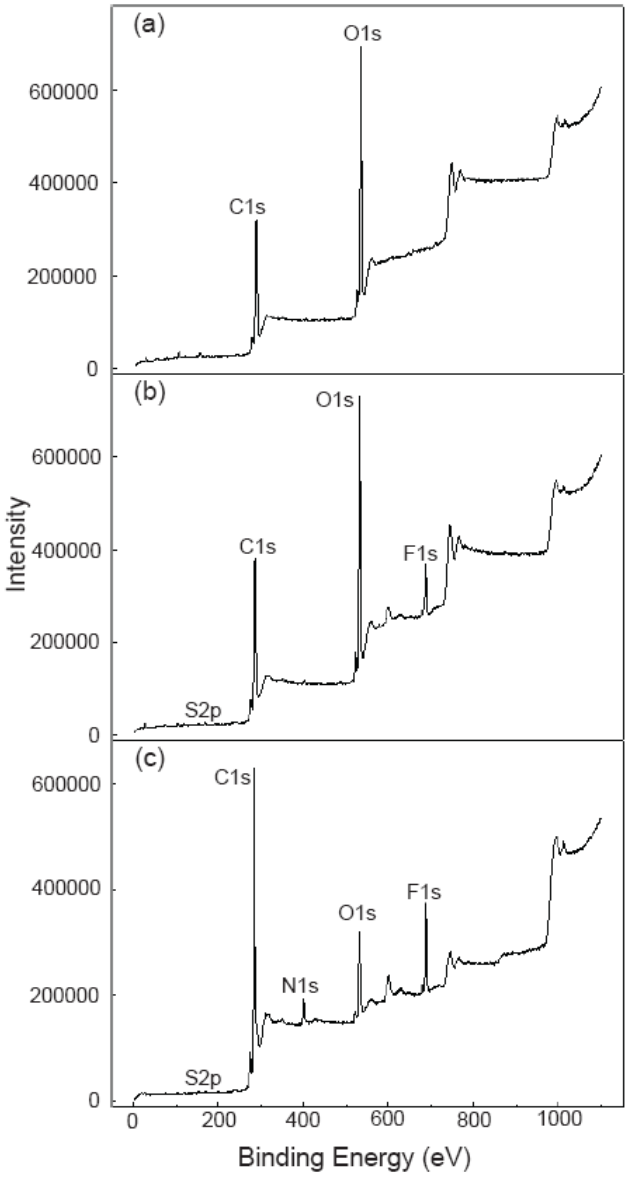
(a)
O1s
C1s
600000
400000
200000
0
(b)
O1s
C1s
F1s
S2p
600000
400000
200000
0
Intensity
(c)
C1s
F1s
O1s
N1s
S2p
600000
400000
200000
0
0
200
400
600
800
1000
Binding Energy (eV)

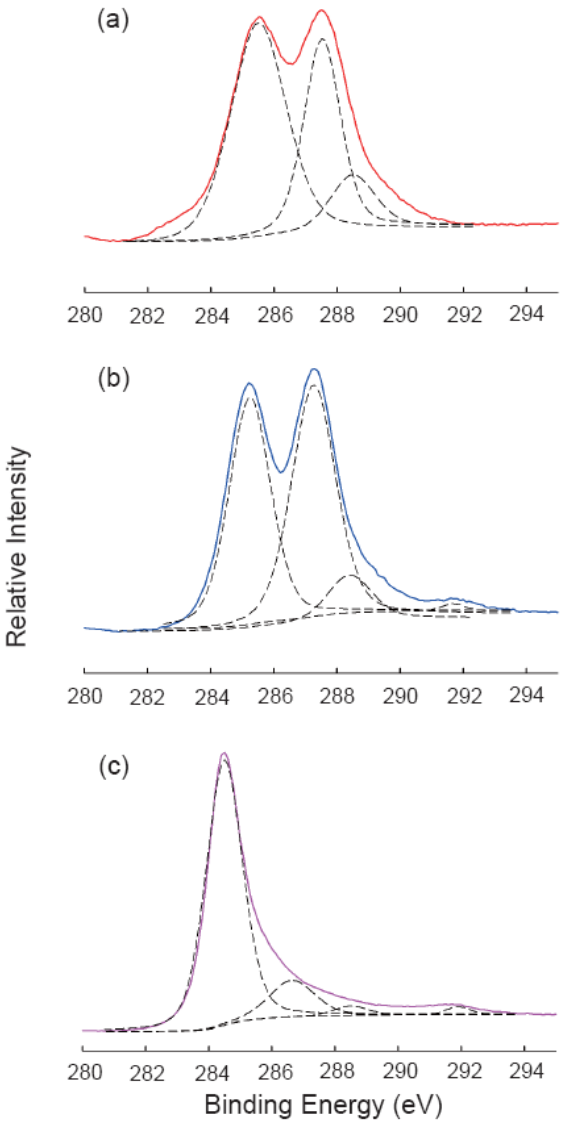

Figure S3. (A) XPS survey spectra and (B) C1s XPS spectra of (a) GO, (b) GON, and (c) RGON.

The XPS data was used to investigate the surface chemical states of GO, GON, and RGON as shown in Figure S4. The survey scan XPS spectra showed that the presence of the Nafion was clearly confirmed on both of the GO sheets after sonic treatment with the Nafion and the RGON hybrids after the hydrazine treatment from the elemental analysis of the Nafion, such as F 1s and S 2p. Through fitting the C 1s of GO, the separated three peaks of C-C (285.5 eV), C-O (287.4 eV), and C=O (288.4 eV) were observed, which is consistent with previous report.[2] In particular, the C1s XPS spectrum of

GON was split into four peaks (285.2 eV, 287.3 eV, 288.4 eV, and 291.6 eV). The three peaks at 285.2 eV, 287.3 eV, and 288.4 eV were attributed to the carbon atoms in different functional groups of GOs. The peak at 291.6 eV was assigned to the CF_2, CF-O, and CF_2-O groups from Nafion, which is consistent with the results reported by Noda *et al.* group.[3] After reduction of GON, most of the C-O (286.7 eV) and the C=O (288.5 eV) of GON have been removed by reduction and the peak at 291.8 eV was remained.

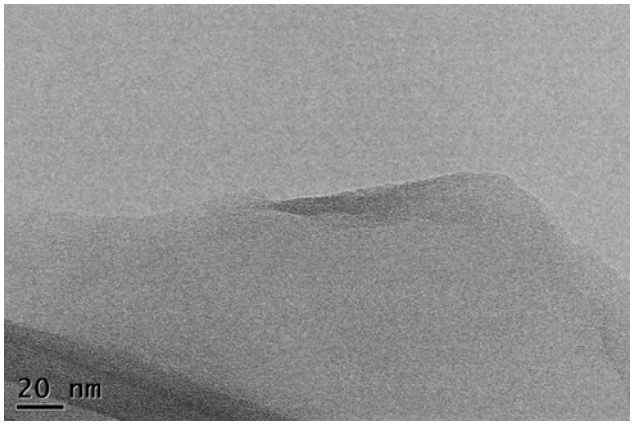

(A)

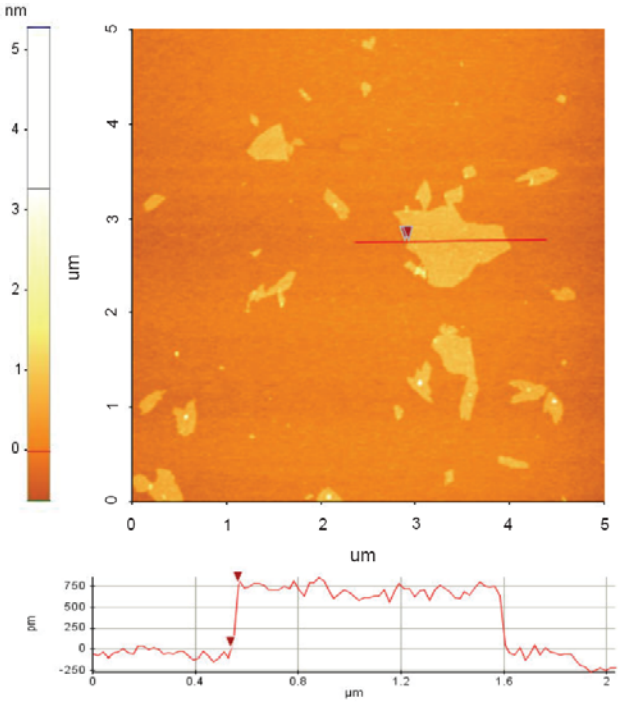

(B)

Figure S4. (A) TEM image and (B) Non-contact mode AFM image of exfoliated GO.

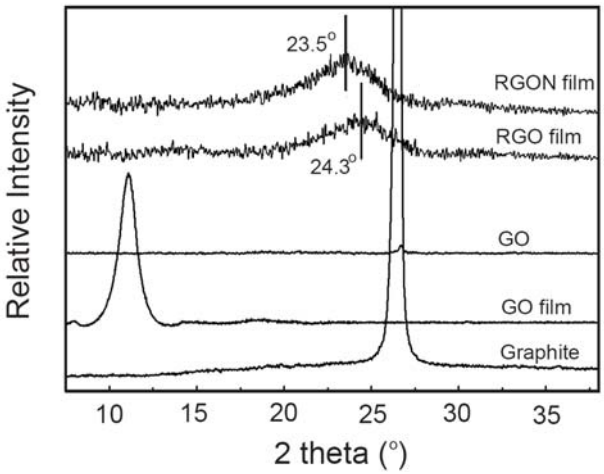

Figure S5. XRD patterns of graphite powder, GO powder, GO film, RGO film, and RGON film.

XRD results demonstrate the intercalation of Nafion into the interlayer of RGO sheets, resulting in an expansion of the (002) inter-planar spacing. The GO paper had a distinct peak at 11.2° corresponding to a d-spacing of 7.97 Å, based on the Bragg spacing equation: $n\lambda=2d\sin\theta$ his result was consistent with an increase in the interlayer spacing due to the water molecules between GO sheets. The RGO film obtained from the reduction reaction in bisolvent had a characteristic peak at around 24.3° (3.66 Å), close to but certainly larger than most d-spacings of graphite (3.35 Å).[4] The RGON paper had a higher d-spacing (3.79 Å) than the RGO paper due to Nafion intercalation into the interlayer of the RGO sheets.

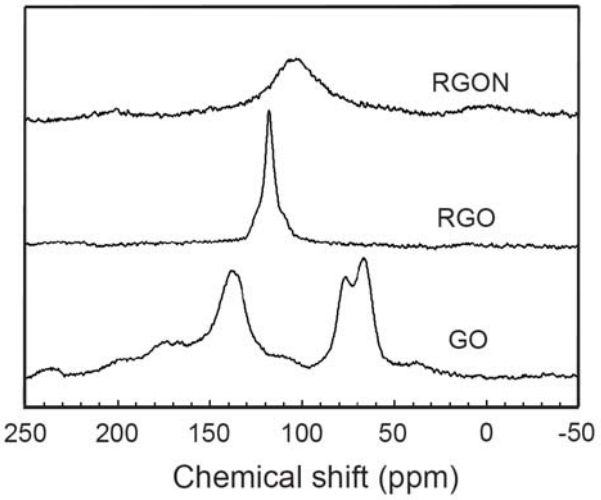

Figure S6. Solid-state ^{13}C MAS NMR spectra of GO, RGO, and RGON hybrid.

Because ^{13}C MAS NMR spectra reflect the chemical environment of materials, the interactions between Nafion and GO or RGO can be elucidated. GOs exhibit three distinct resonances: the bands of un-oxidized sp^2 carbons at 138 ppm, the hydroxyl groups at 76 ppm, and the epoxide groups at 66 ppm.[5,6] In contrast, RGO showed the disappearance of bands related to the oxygenated and carbonyl carbons and the shift of the sp^2 band to 119 ppm. The change in the chemical environment from GO to RGO induced the band to shift from 138 ppm to 119 ppm.[5] The emergence of a broad resonance in RGON at 105 ppm was attributed to the hydrophobic interactions between the conjugated carbons of RGO and CF_2 groups of Nafion.

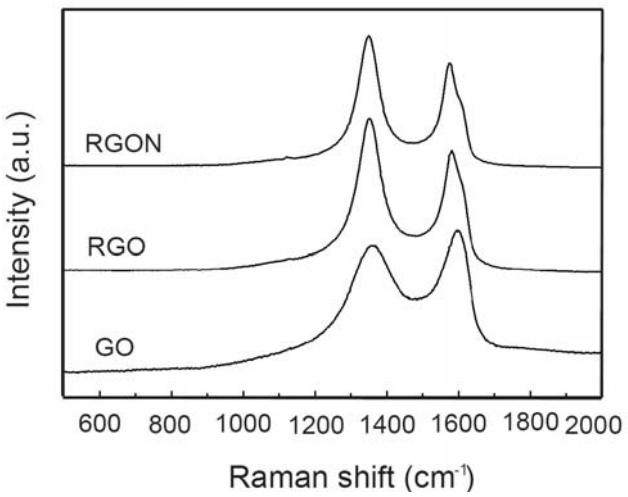

Figure S7. Raman spectra of GO, RGO, and RGON.

The Raman spectrum of GO showed two prominent bands at 1600 cm^{-1} and 1356 cm^{-1}, which correspond to the G and D bands. In particular, the dominant D peak is indicative of the existence of defects such as hydroxyl and epoxide groups in the in-plane sp^2 conjugated structure of functionalized GO due to extensive oxidation.[7] The higher ratio of D/G intensity in RGO than in GO indicates the restoration of conjugation by means of the decrease in the average size of the sp^2 domains of the GOs during the reduction.[5] The D/G intensity ratio of in RGON was comparable to that in RGO, whereas the bands of RGO at 1579 cm^{-1} and 1350 cm^{-1} were shifted to 1572 cm^{-1} and 1347 cm^{-1} for RGON, and the band width was broadened due to the specific interactions between RGO and Nafion.


6
7
8
9
10
11
12
13
14
15
16
17

(A)

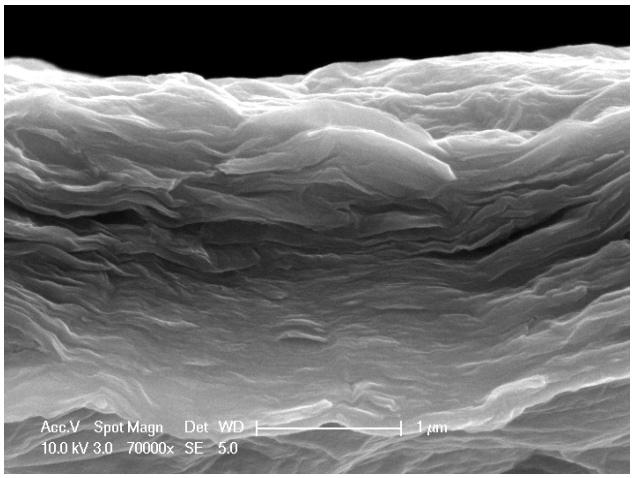
Acc.V Spot Magn Det WD 1 μm
10.0 kV 3.0 70000x SE 5.0

(B)

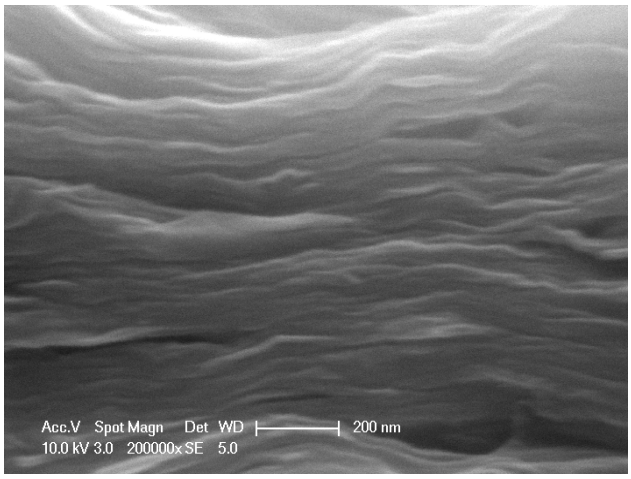

(C)

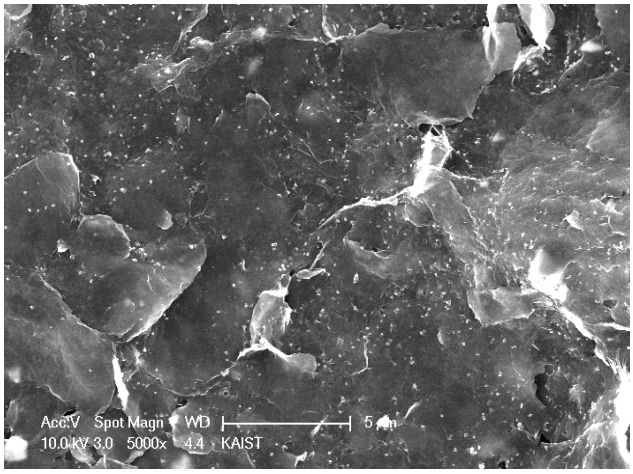

(D)

Figure S8. (A) Photograph of free-standing RGON films. (B, C) SEM images of the cross-section of RGON film. (D) SEM image of the surface of RGON film.

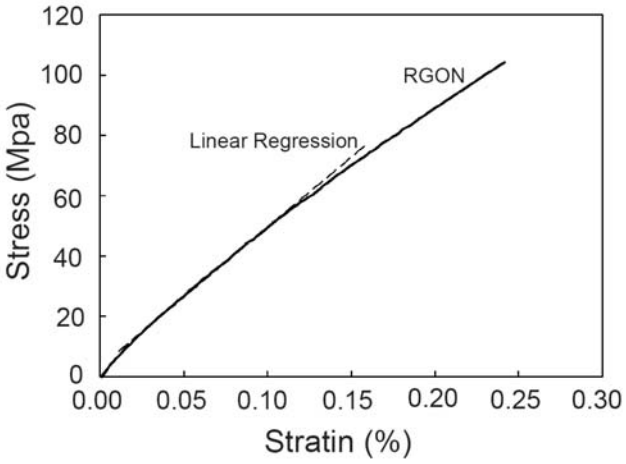

Figure S9. Typical stress-strain curve of RGON film.

Table S1. Performance of various sensors

Sensor Type	Substrate	Sensitivity (nA/μM)	Linear range	Response time (sec)	Limit of detection (× μM)
RGON with amperometric response	paraoxon	10.7	2–20μM	~3	0.13
Thick-film with amperomeric reponse[8]	Methyl parathion	2.83	5–40μM	~10	0.07
	paraoxon	1.67	5–40μM	~10	0.09
Gold electrode with amperomeric flow injection[9]	Paraoxon	2.29	1–10μM	~40	0.1
CNT-modified electrode with amperometric flow injection[10]	paraoxon	25	0.25–4μM	~10	3.60

Supplementary References

(1) Xu, Y.; Bai, H.; Lu, G.; Li, C.; Shi, G. Flexible Graphene Films *via* the Filtration of Water-Soluble Noncovalent Functionalized Graphene Sheets. *J. Am. Chem. Soc.* **2008**, *130*, 5856–5857.

(2) Cai, D.; Song, M. Preparation of Fully Exfoliated Graphite Oxide Nanoplatelets in Organic Solvents. *J. Mater. Chem.* **2007**, *17*, 3678–3680.

(3) Zhang, J.; Gao, L.; Sun, J.; Liu, Y.; Wang, Y.; Wang, J.; Kajiura, H.; Li, Y.; Noda, K. Dispersion of Single-Walled Carbon Nanotubes by Nafion in Water/Ethanol for Preparing Transparent Conducting Films. *J. Phys. Chem. C* **2008**, *112*, 16370–16376.

(4) Park, S.; An, J.; Jung, I.; Piner, R. D.; An, S. J.; Li, X.; Velamakanni, A.; Ruoff, R. S. Colloidal Suspensions of Highly Reduced Graphene Oxide in a Wide Variety of Organic Solvents. *Nano Lett.* **2009**, *9*, 1593–1597.

(5) Stankovich, S.; Dikin, D. A.; Piner, R. D.; Kohlhaas, K. A.; Kleinhammes, A.; Jia, Y.; Nguyen, S. T.; Ruoff, R. S. Synthesis of Graphene-based Nanosheets *via* Chemical Reduction of Exfoliated Graphite Oxide. *Carbon* **2007**, *45*, 1558–1565.

(6) Si, Y.; Samulski, E. T. Synthesis of Water Soluble Graphene. *Nano Lett.* **2008**, *8*, 1679–1682.

(7) Yang, D.; Velamakanni, A.; Bozoklu, G.; Park, S.; Stoller, M.; Piner, R. D.; Stankovich, S.; Jung, I.; Field, D. A.; Ventrice Jr., C. A. V.; Ruoff, R. S. Chemical Analysis of Graphene Oxide Films After Heat and Chemical Treatments by X-ray Photoelectron and Micro-Raman Spectroscopy. *Carbon* **2009**, *47*, 145–152.

(8) Mulchandani, A.; Mulchandani, P.; Chen, W.; Wang, J.; Chen, L. Amperometric Thick-Film Strip Electrodes for Monitoring Organophosphate Nerve Agents Based on Immobilized Organophosphorus Hydrolase. *Anal. Chem.* **1999**, *71*, 2246–2249.

(9) Wang, J.; Krause, R.; Block, K.; Musameh, M.; Mulchandani, A.; Schöning, M. J. Flow Injection Amperometric Detection of OP Nerve Agents Based on an Organophosphorus-Hydrolase Biosensor Detector. *Biosens. Bioelectron.* **2003**, *18*, 255–260.

(10) Deo, R. P.; Wang, J.; Block, I.; Mulchandani, A.; Joshi, K. A.; Trojanowicz, M.; Scholz, F.; Chen, W.; Lin, Y. Determination of Organophosphate Pesticides at a Carbon Nanotube/Organophosphorus Hydrolase Electrochemical Biosensor. *Anal. Chim. Acta* **2005**, *530*, 185–189.